Article

What Is Required to Stabilize Al? A Gas-Phase Perspective

Ljiljana Pukar, Katharine Tomlins, Bridgette Duncombe, Hazel Cox, and Anthony J. Stace

J. Am. Chem. Soc., **2005**, 127 (20), 7559-7569• DOI: 10.1021/ja042884i • Publication Date (Web): 30 April 2005

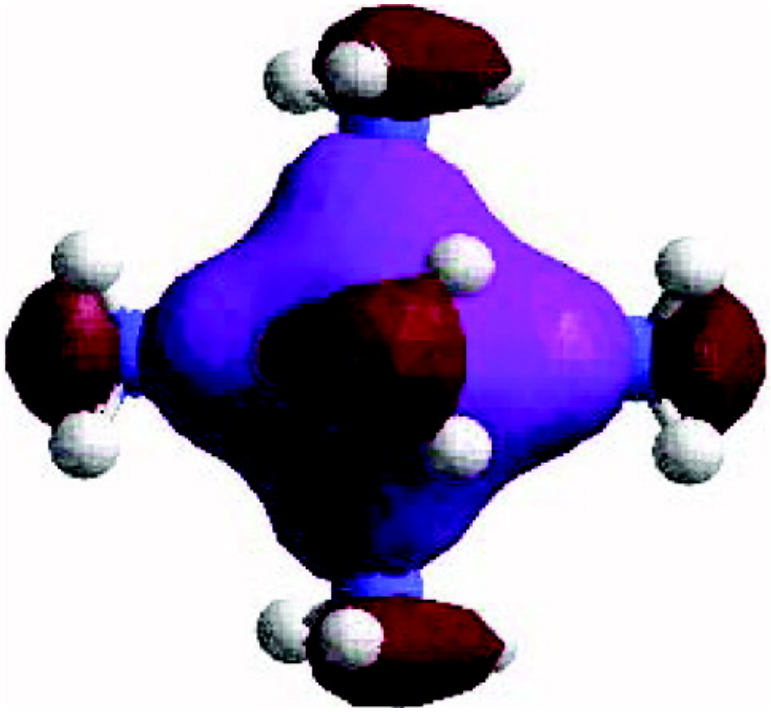

J|A|C|S
ARTICLES
Published on Web 04/30/2005

What Is Required to Stabilize Al^{3+}? A Gas-Phase Perspective

Ljiljana Puškar, Katharine Tomlins, Bridgette Duncombe,§ Hazel Cox,* and Anthony J. Stace*,§

Contribution from the Department of Chemistry, University of Sussex, Falmer, Brighton BN1 9 QJ, U.K.

Received November 25, 2004; E-mail: h.cox@sussex.ac.uk; anthony.stace@nottingham.ac.uk

Abstract: With a combination of experiment and theory (ab initio and DFT), we demonstrate that the Al^{3+} cation can be stabilized in the gas phase using ligands, which have the ability to act as powerful σ electron donors and electron acceptors. The latter property, which implies that electron density from the aluminum cation moves into ligand antibonding orbitals, has not previously been considered significant when accounting for the behavior of Al^{3+}. Of the three ligands identified as falling into the above category, acetonitrile appears to form the most stable complexes in the gas phase, which is in accord with the long established fact that solid-state complexes with Al^{3+} are readily isolated. From the results, it is suggested that chain or ring compounds containing the $-C\equiv N$ group might act as successful sequestering agents for Al^{3+} from aqueous solutions.

I. Introduction

Aluminum is the most abundant metallic element in the Earth's crust, and yet its ionic chemistry is relatively unexplored because of the ease with which Al^{3+} complexes undergo hydrolysis in aqueous solution. With an ionic radius of just 0.53 Å, Al^{3+} is generally considered to be a very hard acid and appears to require complexation with equally hard bases if the latter are to compete effectively with the hydrolysis reaction. Suitable bases frequently take the form of oxygen-containing ligands that are capable of chelating the metal ion.[1,2]

Interest in the biochemistry of aluminum centers on the toxicity of the metal,[3] Al^{3+} and its compounds have no known beneficial biological functions, but the cation has gained prominence through a possible link to Alzheimer's disease.[4] The high Lewis acidity of Al^{3+}, combined with a slow rate of ligand exchange, means that the cation is able to compete efficiently with other metal ions for preferential coordination.[5] In the case of magnesium, replacement by Al^{3+} could inhibit a number of Mg^{2+}/enzyme-induced phosphate transfer reactions.[6] Likewise, Al^{3+} has the potential to replace Fe^{3+} in a variety of coordination sites, but whereas iron is an essential component of almost all biological systems, the presence instead of aluminum is more likely to be disruptive.[7] There has also been some discussion of the interplay between silicon and aluminum in aqueous chemistry and evidence provided of how a deficiency of the former can enhance the uptake and toxicity of aluminum.[8]

What differentiates the geochemistry of Al(III) from the potential for incorporation into biochemical processes is the ability of the metal ion to form stable Al(III)−ligand complexes that are soluble.[1] To better understand the chemical and physical factors that influence the coordination of Al^{3+} to a variety of ligand (L) sites, experiments have been undertaken that explore the stability of $[AlL_N]^{3+}$ complexes in the gas phase. A number of recent experiments of this nature have demonstrated that it is possible to stabilize multiply charged states of metal ions through an appropriate choice of ligands.[9] In some instances, unusual or unexpected charge states can be observed by virtue of the collision-free environment within which the experiments are performed. Of the complexes studied to date, the majority have been doubly charged; however, results from gas phase experiments on triply charged cation complexes are beginning to emerge.[10−16] The majority of these recent experiments have matched metals with low third ionization energies (3rd IE) with aprotic ligands, namely, acetone, dimethyl sulfoxide (DMSO), dimethyl formamide, and acetonitrile.[10−16] The only protic solvent found to bind successfully with M^{3+} cations in the gas phase is aldol;[12] however, this molecule, like acetone, could coordinate via carbonyl groups.[11]

* Contact H.C. for theory and A.J.S. for experimental information.
§ Present address: School of Chemistry, The University of Nottingham, University Park, Nottingham NG7 2RD.

(1) Orgiv, C. In *Coordination Chemistry of Aluminum*; Robinson, G. H., Ed.; VCH Publishers: New York, 1993; pp 85−121.
(2) Yokel, R. A. *Coord. Chem. Rev.* **2002**, *228*, 97−113.
(3) William, R. J. P. *Coord. Chem. Rev.* **2002**, *228*, 93−96.
(4) Yokel, R. A. *Neurotoxicology* **2000**, *21*, 813.
(5) Burgess, J. *Metal Ions in Solution*; John Wiley: London, 1978.
(6) Kaim, W.; Schwederski B. *Bioinorganic Chemistry: Inorganic Elements in the Chemistry of Life*; John Wiley: London, 1994.
(7) Schmitt, W.; Jordan, P. A.; Henderson, R. K.; Moore, G. R.; Anson, C. E.; Powell, A. K. *Coord. Chem. Rev.* **2002**, *228*, 115−126.
(8) Birchall, J. D. *Chem. Brit.* **1990**, 141.
(9) Stace, A. J. *J. Phys. Chem. A* **2002**, *106*, 7993−8005.
(10) Blades, A. T.; Jayaweera, P.; Ikonomou, M. G.; Kebarle, P. *Int. J. Mass Spectrom. Ion Processes* **1990**, *101*, 325−336.
(11) Walker, N. R.; Stace, A. J.; Woodward, C. A. *Int. J. Mass Spectrom.* **1999**, *188*, 113−119.
(12) Shvartsburg, A. A. *J. Am. Chem. Soc.* **2002**, *124*, 7910.
(13) Shvartsburg, A. A. *J. Am. Chem. Soc.* **2002**, *124*, 12343−12351.
(14) Shvartsburg, A. A. *Chem. Phys. Lett.* **2002**, *360*, 479−486.
(15) Shvartsburg, A. A.; Jones, R. C. *J. Am. Soc. Mass Spectrom.* **2004**, *15*, 406−408.
(16) Cheng, Z. L.; Siu, K. W. M.; Guevremont, R.; Berman, S. S. *Org. Mass Spectrom.* **1992**, *27*, 1370.

The problems encountered in performing these experiments are easy to visualize; the average ionization energy (IE) of an organic ligand is ~10−11 eV, whereas the 2nd or 3rd IE of a metal could be >20 eV. Hence, there is a considerable energy difference between the two, and attempts to form multiply charged metal−molecule complexes are not always successful. For the case of aluminum, the 2nd and 3rd IEs are 18.75 and 28.44 eV, respectively, which means that with a potential energy difference of ~18 eV, there is considerable inducement for Al^{3+} to undergo charge transfer (reduction) to Al^{2+}. Relevant to the work discussed here is the observation by Shvartsburg that Al^{3+} can be stabilized in the gas phase[13] in $[Al(DMSO)_N]^{3+}$ complexes. These are prepared via electrospray and their fragmentation patterns analyzed by use of mass spectrometry.

Shvartsburg has proposed that at least three DMSO molecules are required to prevent charge transfer;[13] a result that is supported by very recent DFT calculations by El-Nahas et al.[17] However, dimethyl sulfoxide does not meet the criterion of being a particularly hard base that could match the hard acidity normally attributed to Al^{3+}.[18] To explore this anomaly further, we have attempted to prepare stable gas-phase complexes between Al^{3+} and a variety of ligands with varying physical properties. The ligands range from those previously identified with the chemistry of Al^{3+} in the condensed phase,[19−23] such as acetonitrile, through to more esoteric ligands, such as argon and CO_2, which in earlier gas-phase experiments have been shown to successfully stabilize uncommon oxidation states, such as Ag(II) and Au(II).[24,25] Although many of the ligands explored are simple when compared to those previously associated with the aqueous chemistry of Al^{3+},[1,2] the range does cover those that stabilize Al^{3+} and those that do not. An advantage of examining ligands containing few atoms is that they are amenable to theoretical analysis. Therefore, as part of our discussion of the criteria for stability, use is made of an electrostatic model that takes account of the physical properties of the ligands (IE, dipole moment, and polarizability) and represents charge transfer as a curve-crossing process.[25,26] Possible reduction to either Al^{2+} or Al^{+} is then determined by the location of the appropriate crossing point. However, at a quantitative level, the electrostatic model alone fails to provide an understanding of all the molecular interactions responsible for stabilizing Al^{3+}. For a more detailed analysis, use is made of ab initio and density functional (DFT) methods, and it is here that the level of detail afforded by the calculations is aided by the simplicity of the ligands. The calculations reveal the presence of low-lying molecular orbitals between Al^{3+} and successful σ bonding ligands. These orbitals are responsible for transferring the equivalent of up to one unit of charge (1e) from the ligands to the metal cation. However, electron transfer is not all one-way; a successful ligand appears to require the ability to accept a modest amount of electron density back from the metal cation into low-lying antibonding molecular orbitals. Again, such behavior is not characteristic of a typical "hard" base.

II. Experimental Section

A detailed description of the instrumentation used for generation, resolution, and detection of the cluster beam has been provided in previous publications.[24,27] Briefly, pulses of argon carrier gas at a pressure between 30 and 40 psi are passed through a custom-built reservoir containing solvent in its liquid state, enabling solvent molecules to enter the argon flow. Since many of the molecules studied are quite volatile, it was frequently necessary to cool the reservoir in ice to maintain the required concentration of solvent over an extended period of time. The mixture of argon and solvent vapor was then subjected to supersonic expansion through a pulsed conical nozzle, followed by collimation 2 cm downstream by a 1 mm diameter skimmer. Midway between the expansion chamber and the mass spectrometer, the cluster beam passed over the mouth of a high temperature effusion cell (DCA Instruments, EC-40−63-21) equipped with a crucible of pyrolytic boron nitride. Particular care had to be taken to avoid the problems of corrosion associated with liquid aluminum, with each crucible typically lasting for approximately 40 h of experimentation. To maximize the surface area of metal, the cell was positioned at a slight angle (≅30°) with respect to the vertical. Metal vapor was allowed to diffuse into the flight tube in order to create a region where the vapor and the cluster beam could interact. All previous experiments using the "pick-up" technique have shown that the presence of clusters in the beam of the form Ar_NL_M is essential for the successful generation of neutral ML_K complexes.

Signal intensities measured on the apparatus over a series of experiments have suggested that the optimal partial pressure of metal vapor is between 10^{-1} and 10^{-2} Torr. Above this pressure, disruption of the cluster beam results in reduced signal intensity, and at lower pressures, the signal of metal/solvent clusters decreases. For aluminum, the above partial pressure was estimated from the observation that the effusion cell operated most effectively when the temperature was held at 1150° C, as measured with a standard C-type thermocouple. Formation of neutral metal/solvent clusters results from the collision of metal atoms with argon/solvent clusters, with the energy from the collision being dispersed by the ejection of argon atoms. This latter step is essential since collisions might otherwise form species with high internal energies, which would break up immediately. A shutter at the exit of the effusion cell was used to confirm the identity of clusters containing aluminum, and where a survey was performed of the relative intensities of parent ions of a given series, the difference was taken between signal intensities with the shutter open and closed. This approach removed any contribution from background signal that was not dependent on material originating from the effusion cell.

The neutral metal/solvent clusters were ionized by 100 eV electrons within the ion source of a high resolution, double focusing mass spectrometer (VG ZAB-E) and were then accelerated by a potential of +5 kV. After passing through a field free region, ions were selected according to their mass/charge ratio in a magnetic sector. A second field free region separated the magnetic sector from an electrostatic analyzer (ESA), and the presence of a gas cell in this region permitted the collisional activation (CA) of size-selected parent ions. For all of the stable complexes discussed here, CA fragmentation processes were examined as a mechanism for confirming the composition and m/z assignment of the ion. The general approach used to generate complexes

(17) El-Nahas, A. M.; Xiao, C.; Hagelberg, F. *Int. J. Mass Spectrom.* **2004**, *237*, 47.
(18) Fraústo da Silva, J. J. R.; Williams, R. J. P. *The Biological Chemistry of the Elements*; OUP: Oxford, 2001.
(19) Beattie, I. R.; Jones, P. J.; Howeard, J. A. K.; Smart, L. E.; Gilmore, C. J.; Akitt, J. W. *J. Chem. Soc., Dalton Trans.* **1979**, 528.
(20) Babian-Kibala, E.; Chen, H.; Cotton, F. A.; Daniels, L. M.; Falvello, L. R.; Schmid, G. Yao, Z. *Inorg. Chim. Acta* **1996**, *250*, 359−364.
(21) Suzuki, H.; Ishiguro, S. *Acta Crystallogr.* **1998**, *C54*, 586−588.
(22) Bekaert, A.; Barberan, O.; Kaloun, E. B.; Rabhi, C.; Danan, A.; Brion, J. D.; Lemoine, P. *Z. Kristallogr.: New Cryst. St.* **2003**, *217*, 128.
(23) Mooy, J. H.; Krieger, W.; Heijdenrijk, D.; Stam, C. H. *Chem. Phys. Lett.* **1974**, *29*, 179.
(24) Walker, N. R.; Wright, R.; Stace, A. J. *J. Am. Chem. Soc.* **1999**, *121*, 4837−4844.
(25) Walker, N. R.; Wright, R. R.; Barran, P. E.; Murrell, J. N.; Stace, A. J. *J. Am. Chem. Soc.* **2001**, *123*, 4223−4227.
(26) Walker, N. R.; Dobson, M.; Wright, R. R.; Barran, P. E.; Murrell, J. N.; Stace, A. J. *J. Am. Chem. Soc.* **2000**, *122*, 11138−11145.
(27) Wright, R. R.; Walker, N. R.; Firth, S.; Stace, A. J. *J. Phys. Chem. A* **2001**, *105*, 54−64.

results in a wide range of ions being observed, many of which have nominal *m*/*z* values that coincide with the ions of interest. By combining the fragmentation pattern with other factors, such as calibrating the mass scale with argon cluster ions and confirming a dependence on oven temperature, it is possible to make accurate *m*/*z* assignments. CA processes were promoted by introducing $\sim 10^{-6}$ mbar of air into the collision cell, and fragments were identified by scanning the ESA in the form of a MIKE (Mass-analyzed Ion Kinetic Energy) scan.[28] These scans were performed on triply charged ions with kinetic energies of 15 keV, which allowed for straightforward detection and verification of fragment ions resulting from both neutral ligand loss and Coulomb explosion that accompanies charge transfer. Final ion detection took place at a Daly detector, where phase-sensitive detection was facilitated by a Stanford Research Systems SR850 lock-in amplifier.

III. Computational Details

Results from two separate computational methods have been used to provide complementary information on the structure and electron populations of Al^{3+} complexes. Complexes of acetonitrile, pyridine, DMSO, acetone, carbon dioxide, and ammonia with Al^{3+} ($[AlL_N]^{3+}$, $N = 1-6$) have been investigated using both density functional theory (DFT), as implemented in the Amsterdam Density Functional (ADF) code,[29] and Hartree−Fock/DFT, as implemented in Gaussian 98.[30] For the ADF calculations, the numerical integration procedure of te Velde and Baerends was applied.[31] Energies of the individual structures were calculated using the local density approximation (LDA) from Vosko et al.,[32] and the nonlocal exchange correction of Becke[33] and the nonlocal correlation correction of Perdew[34] were applied to the LDA density. A triple-ζ Slater-type-orbital basis set with a polarization function (TZP in ADF) was used to describe the valence electrons of each atom. The core atomic orbitals of Al were set as [Ne] and treated with the frozen core approximation. The 1s orbitals of carbon, nitrogen, oxygen, and sulfur were similarly treated as frozen cores. The Gaussian 98 calculations were performed at the B3LYP/6-31G*//HF/6-31G* level of theory, and vibrational frequencies calculated at the HF/6-31G* level were routinely checked to confirm that the structures were energy minima. Gaussian 98 was also used to undertake a Natural Bond Orbital (NBO)[35] analysis of the distribution of electrons between Al^{3+} and single ligands. From the NBO data, a natural population analysis (NPA) was also undertaken and used to determine the charge on each atom.

Since Gaussian 98 was used to confirm the minima and to perform the NBO analysis, the results presented are primarily those from B3LYP/6-31G**//HF/6-31G* calculations. The energy decomposition facility within ADF2003 was used to compare the degree of electrostatic bonding within complexes and to perform a full molecular orbital fragment analysis on the $N = 4$ structures. In general, the agreement between optimized structures calculated using the two methodologies was good. A qualitative summary of the structural results of the $[AlL_N]^{3+}$ ions is as follows: $N = 1$ linear; $N = 2$ structures were either staggered ($\approx D_{3d}$) or eclipsed ($\approx D_{3h}$); $N = 3$ structures were trigonal planar; $N = 4$ structures were approximately tetrahedral; for $N = 5$, the preferred geometry was trigonal bipyramidal, and most of the $N = 6$ structures were pseudo-octahedral. The Gaussian (HF) bond lengths were within 2% of the ADF (BP86) results. Notable exceptions were as follows: $[Al(DMSO)_{N=1}]^{3+}$ dissociated when using ADF (BP86). For $[Al(py)_{N=5 \text{ or } 6}]^{3+}$, Gaussian calculations predicted that the fifth (and sixth) ligands were pushed out to a distance of 4.687 Å (and 5.059 Å for the fifth and sixth ligands in $[Al(py)_6]^{3+}$), leaving behind a tetrahedral motif. Vibrational analysis confirmed each of these structures to be true minimum.

Table 1. Summary of Results Following Attempts to Prepare Stable $[AlL_N]^{3+}$ Complexes in the Gas Phase[a]

ligand	stable ?	IE[g] (eV)	α[g] (Å^3)	μ (D)[g]	R_c (Å)	PA (kJ mol^{-1})
water	no	12.61	1.45	1.85	2.2	697
ammonia	no	10.7	2.26	1.47	2.2	853
CO_2	no	13.8	2.91	0	2.4	548
THF	no	9.41	~6	1.75	2.4	822
argon	no	15.76	1.6	0	2.5	371
acetone	*b*	9.7	6.39	2.7	2.5	823
CS_2	no	10.08	8.74	0	2.5	699
benzene	no	9.3	10.32	0	2.6	759
2-butanone	no	9.51	8.13	2.78	2.6	836
diethyl ether	no	9.51	8.73	1.15	2.6	828
urea[c,d]		9.9	5.3	3.57	2.5	874
DMF[c,e]	no	9.13	7.91	3.86	2.6	887
DMSO[f]	**yes**	**9.10**	**8.0**	**3.96**	**2.6**	**834**
pyridine	**yes**	**9.3**	**9.5**	**2.2**	**2.6**	**924**
acetonitrile[s]	**yes**	**12.2**	**4.40**	**3.44**	**2.6**	**788**

[a] Also listed are: (i) the constants used in calculating electrostatic potentials between Al^{3+}, the ligands, and their charge-transfer products; (ii) the curve crossing point, R_c, calculated from the electrostatic model; and (iii) proton affinities, PA, for each of the ligands. Ligands that are successful at stabilizing Al^{3+} are shown in bold. [b] On several separate occasions, there appeared to be experimental evidence for the existence of $[Al(\{CH_3\}_2CO)_N]^{3+}$ complexes; however, the fragmentation data were never sufficiently reproducible to be conclusive. [c] Crystallographic evidence available regarding the formation of a stable structure between this molecule and Al^{3+}.[21−23] [d] No gas-phase experiments were undertaken with this molecule. [e] Dimethyl formamide. [f] Dimethyl sulfoxide; gas-phase results taken from ref 13. [g] IE: ionization energy; D: dipole moment; α: polarizability.

IV. Results and Discussion

(a) Summary of Experimental Data. Table 1 shows the outcome of the experimental studies in terms of successes and failures to generate and observe stable triply charged cation complexes with a wide range of ligands. The term "ligands" is used in its broadest sense, and only those that have low molecular mass are surveyed here because a requirement of the current experimental procedure is that ligands are volatile. Thus, previous experiments have ruled out the use of dimethyl sulfoxide because of its high boiling point,[26] and we have relied on the observations made by Shvartsburg for that particular result.[13] Likewise, the apparatus will not permit experiments on some of the more complex bidentate ligands that have been shown to stabilize Al^{3+} in the condensed phase.[1,2] However, even within these restrictions, the successful ligands that have been identified permit discussion of those molecular properties required to stabilize the trication. By identifying simple Lewis bases that are capable of stabilizing Al^{3+}, it becomes possible to undertake theory on systems that are tractable, and this provides an opportunity to determine precisely what molecular properties are required of a ligand to bind successfully to the ion.

(28) Cooks, R. G.; Beynon, J. H.; Caprioli, R. M.; Lester, G. R. *Metastable Ions*; Elsevier: Amsterdam, 1973.
(29) ADF 2003 Theoretical Chemistry, Vrije Universiteit, Amsterdam; \www: scm.com.
(30) Frisch, M. J.; Trucks, G. W.; Schlegel, H. B.; Scuseria, G. E.; Robb, M. A.; Cheeseman, J. R.; Zakrzewski, V. G.; Montgomery, J. A.; Stratmann, R. E.; Burant, J. C.; Dapprich, S.; Millam, J. M.; Daniels, A. D.; Kudin, K. N.; Strain, M. C.; Farkas, O.; Tomasi, J.; Barone, V.; Cossi, M.; Cammi, R.; Mennucci, B.; Pomelli, C.; Adamo, C.; Clifford, S.; Ochterski, J.; Petersson, G. A.; Ayala, P. Y.; Cui, Q.; Morokuma, K.; Malick, D. K.; Rabuck, A. D.; Raghavachari, K.; Foresman, J. B.; Cioslowski, J.; Ortiz, J. V.; Stefanov, B. B.; Liu, G.; Liashenko, A.; Piskorz, P.; Komaromi, I.; Gomperts, R.; Martin, R. L.; Fox, D. J.; Keith, T.; Al-Laham, M. A.; Peng, C. Y.; Nanayakkara, A.; Gonzalez, C.; Challacombe, M.; Gill, P. M. W.; Johnson, B. G.; Chen, W.; Wong, M. W.; Andres, J. L.; Head-Gordon, M.; Replogle, E. S.; Pople, J. A. *Gaussian 98*, revision A.7; Gaussian, Inc.: Pittsburgh, PA, 1998.
(31) te Velde G.; Baerends, E. J. *J. Comput. Phys.* **1992**, *99*, 84.
(32) Vosko, S. H.; Wilk, L.; Nusair, M. *Can. J. Phys.* **1980**, *58* 1200.
(33) Becke, A. D. *Phys Rev. A* **1988**, *38*, 3098.
(34) Perdew, J. P. *Phys Rev. B* **1986**, *33*, 8822.
(35) Carpenter, J. E.; Weinhold, F. *J. Mol. Struct. (THEOCHEM)* **1988**, *169*, 41.

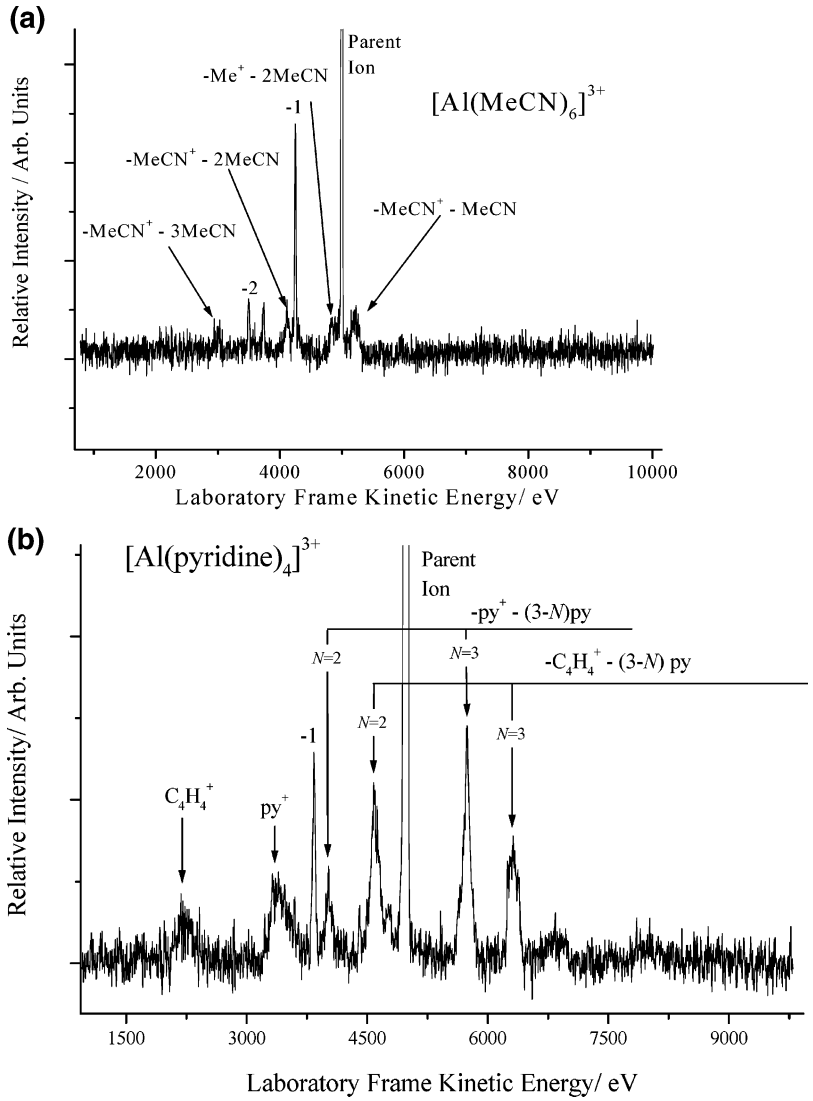

Figure 1. (a) Fragmentation pattern recorded following the collisional activation of $[Al(py)_4]^{3+}$ with air at $\sim 10^{-6}$ mbar. Charge transfer peaks are easily recognized from their increased width due to Coulomb explosion; (b) as for (a), but following the collisional activation of $[Al(MeCN)_6]^{3+}$.

As can be seen from the results, three of the ligands sampled are capable of forming stable Al^{3+} species, namely, acetonitrile, pyridine (py), and DMSO. To confirm these assignments, Figure 1 shows two examples of fragmentation patterns recorded following the collisional activation of $[Al(py)_4]^{3+}$ and $[Al(MeCN)_6]^{3+}$. As already discussed, these measurements are an integral part of the verification process in the assignment of an *m*/*z* value for the ions. However, the results also provide important information on the competition between loss of neutral molecules and charge-transfer routes; in effect, they provide a measure of the ease with which Al^{3+} complexes undergo reduction. From the two examples shown, it can be seen that for the smaller complex, $[Al(py)_4]^{3+}$ shown in Figure 1a, a significant fraction of the reaction products involve charge transfer accompanied by molecular fragmentation. Two charge-transfer channels appear dominant, and these are

$$[Al(py)_4]^{3+} \rightarrow [Al(py)_N(H)CN]^{2+} + C_4H_{4(5)}^{+} + (3\text{-}N)py \quad (1)$$

and

$$[Al(py)_4]^{3+} \rightarrow [Al(py)_N]^{2+} + py^{+} + (3\text{-}N)py \quad (2)$$

In each case, fragments for $N = 2$ and 3 are observed, and there is evidence of both charged fragments from each reaction. The resolution of the experiment is such that it is not always possible to distinguish between fragments that differ by 1 amu; hence, a product of reaction 1 could be either $[Al(py)_NCN]^{2+}$ or $[Al(py)_NHCN]^{2+}$. Although CN^- (bonding through the carbon atom) can successfully ligate metal ions,[36] the similarity between HCN (bonding through the nitrogen atom) and CH_3CN (see below) means that HCN cannot be ruled out as a possible reaction product. Several of the charge-transfer fragments match those observed by Kohler and Leary following the decay of $[M\cdot(py)_N]^{2+}$ complexes,[37] where M is either Co or Mn. Their superior resolution reveals the presence of minor proton transfer channels, which we are unable to identify. However, none of the spectra presented by Kohler and Leary shows evidence of the comparatively intense metal-containing (H)CN fragment. In support of HCN as a reaction product, we note that Kohler

(36) Cotton, F. A.; Wilkinson, G. W. *Advanced Inorganic Chemistry*; Wiley: London, 1988.
(37) Kohler, M.; Leary, J. A. *J. Am. Soc. Mass Spectrom.* **1997**, *8*, 1124−1133.

and Leary do observe the complementary $(py\text{-}HCN)^+$ ion.[37] However, in a more recent study of $[M(py)_N]^{2+}$ complexes, Shvartsburg concluded that ring destruction accompanied charge transfer to yield the products of the form $MCN^+(py)_{N-1} + C_4H_5^+$.[38] Given that Shvartsburg could assign the MCN^+ product ion, it is possible that fragment ions of the form $[AlCN\cdot(py)_{N-X}]^{2+}$ (for $X = 1$ and 2) are responsible for the charge-transfer features seen in Figure 1a. However, in terms of offering a mechanism for reaction 1, HCN would appear to be a more logical neutral product since there is no obvious route to the formation of $C_5H_5^+$.

Apart from the products associated with reactions 1 and 2 above, the only other reaction pathway that can be identified corresponds to the process

$$[Al(py)_4]^{3+} \rightarrow [Al(py)_3]^{3+} + \text{pyridine} \quad (3)$$

The presence of this reaction would imply that $[Al(py)_3]^{3+}$ is a stable trication, which would support the observation by Shvartsburg[13] that at least three ligands, such as DMSO, are required to stabilize Al^{3+}.

For the six-coordinate $[Al(MeCN)_6]^{3+}$ complex (Figure 1b), the most important fragmentation routes are those involving the loss of neutral molecules:

$$[Al(MeCN)_6]^{3+} \rightarrow [Al(MeCN)_{4,5}]^{3+} + (1,2)MeCN \quad (4)$$

The less intense charge-transfer channels are

$$[Al(MeCN)_6]^{3+} \rightarrow [Al(MeCN)_N]^{2+} + MeCN^+ + (5\text{-}N)MeCN \quad (5)$$

for $N = 2-4$, and

$$[Al(MeCN)_6]^{3+} \rightarrow [Al(MeCN)_NCN]^{2+} + Me^+ + (5\text{-}N)MeCN \quad (6)$$

for $N = 2-4$. As with the pyridine reactions, we are unable to distinguish CN from HCN; however, previous studies by Kohler and Leary[37,39] and Shvartsburg et al.[40] on acetonitrile clustered with a wide range of doubly and triply charged metal cations show evidence of reaction 6. These authors also show the presence of a proton-transfer reaction that accompanies reaction 5, but we are unable to detect (resolve) this. Shvartsburg also identified a similar range of reactions in a study of metal trications in association with acetonitrile.[14] For our purposes, these experimental results confirm that stable triply charged aluminum complexes with both pyridine and acetonitrile being generated in our apparatus. What is not seen in any of the fragmentation patterns shown in Figure 1 is evidence of double charge transfer to yield Al^+, and a semiquantitative interpretation of this absence is given below.

In addition to the positive results obtained from pyridine and acetonitrile, numerous experiments with acetone suggested the presence of $[Al(\{CH_3\}_2CO)_N]^{3+}$ complexes. A previous study with holmium demonstrated that acetone is capable of yielding stable triply charged complexes of the form $[Ho(\{CH_3\}_2CO)_N]^{3+}$.[11] However, none of the fragments arising from collisional activation of the $Al^{3+}/\{CH_3\}_2CO$ complexes could be attributed to acetone fragments of the type seen in the earlier experiments involving Ho^{3+}. Given the difficulties experienced in undertaking this program of experiments, the possibility that $[Al(Me_2CO)_N]^{3+}$ complexes may be stable is not ruled out completely, and we shall return to this system when the ab initio and DFT results are discussed.

Table 1 includes physical properties of the ligands, that is, polarizability and dipole moment, which will have an influence on the magnitude of any electrostatic interaction with Al^{3+}. The final column of Table 1 lists proton affinities (PAs) for the ligands. Since H^+ is the hardest known Lewis acid, some correlation might have been expected between PA and the ability of a ligand to coordinate to Al^{3+}; however, as the results show, there is no obvious relationship. The success of the two nitrogen-containing ligands matches earlier results on Ag(II) in the gas phase,[24] where it was shown that coordination to N has a greater stabilizing influence on the metal ion than when oxygen atoms are involved.

In two earlier studies of doubly charged gas-phase complexes,[25,26] a model based on a consideration of elementary electrostatic interactions[41] has successfully been used to account for differences in behavior seen across a wide range of ligands. The model balanced the ability of various ligands to stabilize a cation against competing interactions that lead to surface crossing and reduction. In a study of the hard acid Mg^{2+}, it was observed that one or more of the following properties on the part of a ligand (dipole moment, polarizability, and ionization energy) could contribute toward stabilizing the cation with respect to charge transfer. Examples could be identified where each property played a significant role in influencing the stability of a particular class of complex.[26] The basic equations that contribute to the electrostatic model when applied to a triply charge ion are

$$E(Al^{3+} - L) = \Delta - \frac{z_A\mu}{4\pi\epsilon_0 r^2} - \frac{{z_A}^2\alpha}{8\pi\epsilon_0 r^4} \quad (7)$$

$$E(Al^{2+} - L^+) = \frac{z_A z_B}{4\pi\epsilon_0 r} - \frac{z_A\mu}{4\pi\epsilon_0 r^2} - \frac{{z_A}^2\alpha}{8\pi\epsilon_0 r^4} \quad (8)$$

where Δ is the difference between the ionization energies of the metal and the ligand, z is the charge on either the acid (A) or the base (B), μ and α are the dipole moment and polarizability of the ligand, respectively, and r is the separation between the cation and the ligand. The fact that the ion-induced dipole term varies as z^2 means that for a purely electrostatic interaction between a cation and a highly polarizable ligand, the importance of this contribution increases rapidly as a function of charge. However, high polarizability is not a property that is normally associated with a hard Lewes base.

The two curves defined by eqs 7 and 8 cross at an internuclear separation defined as R_c, where the potential energy of the attractive $Al^{3+}-$ligand (L) interaction, as represented by eq 7, is balanced by the charge transfer $Al^{2+}-L^+$ interaction, as represented by eq 8. The model provides a description of charge

(38) Shvartsburg, A. A. *Chem. Phys. Lett.* **2003**, *376*, 6−10.
(39) Kohler, M.; Leary, J. A. *Int. J. Mass Spectrom Ion Processes* **1997**, *162*, 17−34.
(40) Shvartsburg, A. A.; Wilkes, J. G.; Lay, J. O.; Siu, K. W. M. *Chem. Phys. Lett.* **2001**, *350*, 216−224.
(41) Maitland, G. C.; Rigby, M.; Smith, E. B.; Wakeham, W. A. *Intermolecular Forces*; Clarendon Press: Oxford, 1981.

transfer in terms of intersecting potential energy curves that either promote or suppress the movement of an electron, but it does not include any of the dynamics of such a process.[42] Previous calculations have shown that the larger the value of R_c, the less probable charge transfer becomes, and the more likely the complex is to be stable.[25,26] A simple diagram depicting eqs 7 and 8 shows the height of the energy barrier to charge transfer and R_c increasing together.[25,26] Of the parameters considered in Table 1, it can be seen that there is some correlation between the value calculated for R_c and the ability of a particular ligand to stabilize Al^{3+}. However, Table 1 also shows that there are at least four ligands for which $R_c \approx 2.6$ Å, but where the corresponding complexes with Al^{3+} have not been observed in our experiments. Also included in Table 1 are two molecules, urea ($R_c \approx 2.5$ Å) and dimethyl formamide ($R_c \approx 2.6$ Å), that are know from crystallographic data to form stable 6-fold coordination complexes with Al^{3+} in the condensed phase.[21,22] No gas-phase experiments were attempted with urea, but there is an obvious discrepancy with dimethyl formamide. Blades et al. were successful in using electrospray to form M^{3+} complexes between lanthanide metals and dimethyl formamide.[10] However, in our case, it is quite possible that, as with DMSO, the vapor pressure of liquid dimethyl formamide is not sufficient to yield large neutral clusters. Given the contradictions that are present in Table 1, it would appear that factors other than purely electrostatic interactions are associated with the stability of these simple Al^{3+} complexes. However, what is encouraging as far, as the electrostatic model is concerned, is that it gives dimethyl formamide the same value for R_c as other successful (gas phase) ligands, and the value calculated for urea is similar to that determined for acetone, which we consider may be capable of stabilizing Al^{3+}.

An equation equivalent to eq 7 can be written for charge transfer to Al^+; however, that has to involve at least two ligands, and calculations show the critical internuclear distances, R_c, are greater than those represented by eqs 7 and 8. Thus, the first curve crossing point encountered by stable Al^{3+} complexes as they move toward the dissociation asymptote yields Al^{2+} as the metal cation charge-transfer product. This may explain the absence of products containing Al^+. Although Shvartsburg observes Al^+ as a product following the collisional activation of Al^{3+} complexes, he attributes its appearance to consecutive charge transfer as a result of high-energy collisions.[13] The above analysis contrasts with the approach used by Tonkyn and Weisshaar[43] where charge-transfer pathways were discussed in terms of collisions between multiply charged metal atoms and single molecules.

(b) Calculations. All three of the successful gas-phase ligands can act as σ donors; however, that fact alone does not distinguish them from the other less successful ligands given in Table 1. Acetonitrile is already known to form stable complexes with Al^{3+} in the condensed phase,[19,20] and complexes with pyridine derivatives are also known. Within the group of trial ligands, possibly the most important distinction with regard to bonding is between DMSO and the ketones; what is it that distinguishes coordination through the oxygen atom of the S═O group from that of the C═O group in 2-butanone and, possibly, acetone? Likewise, the lack of correlation between the data in Table 1 and the proton affinities (PAs) of the molecules concerned indicates that an overlap between lone-pair electrons on the ligand and a vacant s orbital on the cation is not sufficient for stability. For example, the PAs of 2-butanone and DMSO are approximately equal, and that of acetonitrile is ~50 kJ mol^{-1} lower than either. Likewise, the proton affinity of ammonia is higher than that of DMSO, but there is no evidence that ammonia forms stable gas-phase complexes with Al^{3+}. Shoeib et al.[44] noted a discrepancy between the property of a proton when viewed as a hard acid and its behavior in relation to ligands that readily bind to metal cations. They concluded that the character of a metal ion only emerges once it becomes associated with a sufficiently large number (~3) of ligands to delocalize a significant fraction of positive charge away from the metal core.[44] In contrast, proton affinity is a single molecule property, and the proton itself can only coordinate a maximum of two molecules.

To better understand what is required of a ligand to stabilize Al^{3+}, density functional and ab initio calculations have been used to analyze a range of properties associated with a number of the complexes identified in Table 1. In particular, the calculations have focused on $[Al(NH_3)_N]^{3+}$ and $[Al(CO_2)_N]^{3+}$ as examples of unstable complexes, and $[Al(CH_3CN)_N]^{3+}$, $[Al(DMSO)_N]^{3+}$, and $[Al(py)_N]^{3+}$ as examples of stable complexes. In all cases, N covers the range of 1−6. Calculations have also been undertaken on $[Al(Me_2CO)_N]^{3+}$ complexes to establish whether the acetone molecule possesses any of the characteristics we may identify as being required to stabilize Al^{3+}.

Recent calculations by El-Nahas on Mg^{2+} (isoelectronic with Al^{3+}) in association with acetone and DMSO[45] reveal a small difference between the two molecules. Both molecules reduce the charge on the metal cation by pushing electron density into the 3s and 3p orbitals of Mg^{2+}, with the effect being slightly more pronounced for DMSO. Possibly of greater significance are the results of calculations involving Zn^{2+} in association with either acetone or DMSO. In both cases, the complexes gain considerable stability from charge transfer, with up to 0.35e moving from the ligand on to the metal cation. Under these circumstances, acetone appears to be slightly more effective than DMSO at charge transfer, but the Zn^{2+}−DMSO binding energy is considerably larger than that of Zn^{2+}−acetone. However, as noted by Peschke et al., the ability of Zn^{2+}, unlike Mg^{2+}, to undergo sdσ hybridization means that it has more complex interactions with ligands, such as acetone.[46] Calculations by Kaczorowska and Harvey[47] on pyridine in association with Fe^{2+} also show a preference for a σ bonded geometry between the metal ion and the ligand. In contrast, similar calculations on the Fe^{2+}/benzene complex show an obvious preference for a π bonded sandwich structure. Note that from a purely electrostatic viewpoint (Table 1), benzene should be as effective at stabilizing Al^{3+} as pyridine.

If factors other than purely electrostatic interactions influence the stability of Al^{3+} complexes, then these should be revealed by the ab initio and DFT calculations. Figure 2 shows a plot of the net (NPA) charge calculated to reside on the aluminum atom as a function of the number of ligands for each of the six

(42) Ferraudi, G. J. *Elements of Inorganic Photochemistry*; Wiley: New York, 1988.
(43) Tonkyn, R.; Weisshaar, J. C. *J. Am. Chem. Soc.* **1986**, *108*, 7128.
(44) Shoeib, T.; Gorelsky, S. I.; Lever, A. B. P.; Siu, K. W. M.; Hopkinson, A. C. *Inorg. Chim. Acta* **2001**, *315*, 236−239.
(45) El-Nahas, A. M. *Chem. Phys. Lett.* **2002**, *365*, 251−259.
(46) Peschke, M.; Blades, A. T.; Kebarle, P. *J. Am. Chem. Soc.* **2000**, *122*, 10440.
(47) Kaczorowska, M.; Harvey, J. N. *Phys. Chem. Chem. Phys.* **2002**, *4*, 5227.

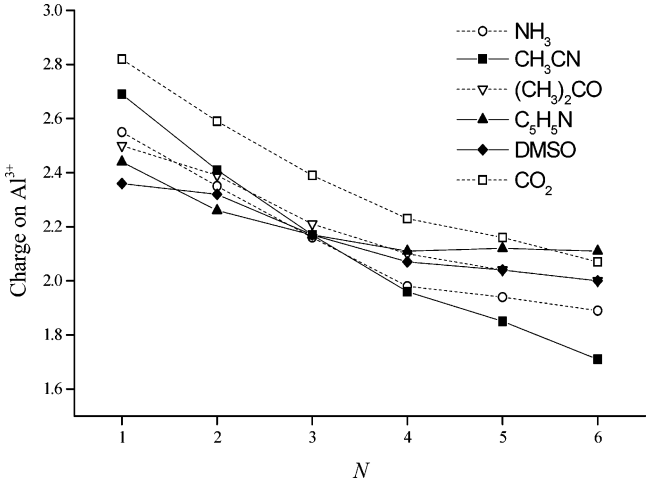

Figure 2. Calculated charge on the aluminum cation in $[AlL_N]^{3+}$ complexes plotted as a function of the number of coordinating ligands (*N*).

molecules under consideration. As can be seen, there are significant departures from the formal 3+ charge notionally associated with the metal atom. The degree of electron donation varies from ~0.2e for a single carbon dioxide molecule to ~1.3e for six acetonitrile molecules, but for all ligands, the general trend is one of increasing electron donation as a function of the *total* number of ligands. There is a limited correlation between the ability of a ligand to neutralize the charge on the metal and the stability of the corresponding complex. For example, for CO_2, electron donation to the cation is low and $[Al(CO_2)_N]^{3+}$ complexes are unstable. Likewise, acetonitrile is a good electron donor, and the corresponding complexes are stable. However, the extent of electron donation from four ammonia molecules (unstable) falls within a group that includes all of the stabilizing ligands (DMSO, pyridine, and acetonitrile). Several of the ligands exhibit a marked change of slope at $N = 4$, suggesting that the optimum geometry for electron donation to Al^{3+} is tetrahedral, and that in larger complexes, increased internuclear separation and/or steric hindrance between ligands may actually impose an *upper* limit on the size of the stable trication that can appear in the gas phase; qualitative evidence in support of this comment is discussed below. The alternative might be to push molecules into the next solvation shell, but such an arrangement is unlikely to be stable in the absence of hydrogen bonding. It is clear that the very small ionic radius of Al^{3+} (0.53 Å) imposes a severe constraint on the ability of the cation to coordinate large molecules, such as pyridine. In contrast, the quasi-linear geometry of acetonitrile makes it an ideal ligand as far as coordination and electron donation are concerned, and may account for the fact that, of the ligands studied, it shows the least change in slope at $N = 4$ in Figure 2. These observations may also account for the success of acetonitrile in forming stable solid-state complexes when $N = 5$ and 6.[19,20]

The values given in Figure 2 for ammonia should also be compared with the ~2+ residual charge calculated by Bock et al.[48] for aluminum in the $[Al(H_2O)_6]^{3+}$ complex. The aqueous coordination of Al^{3+} has been interpreted via calculations on isolated $[Al(H_2O)_N]^{3+}$ complexes in several theoretical studies.[49,50] As with most ROH complexes studied thus far in association with triple charged metal cations,[11] experiments

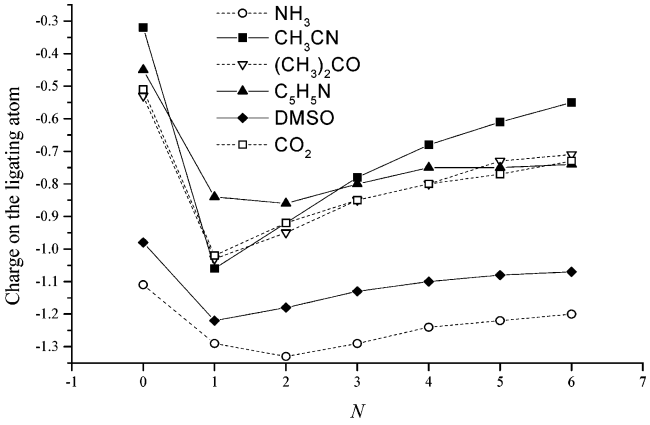

Figure 3. Calculated charge on the ligand atom that is coordinated to the aluminum cation in $[AlL_N]^{3+}$ complexes and plotted as a function of the number of ligands (*N*). Note that the data start at $N = 0$.

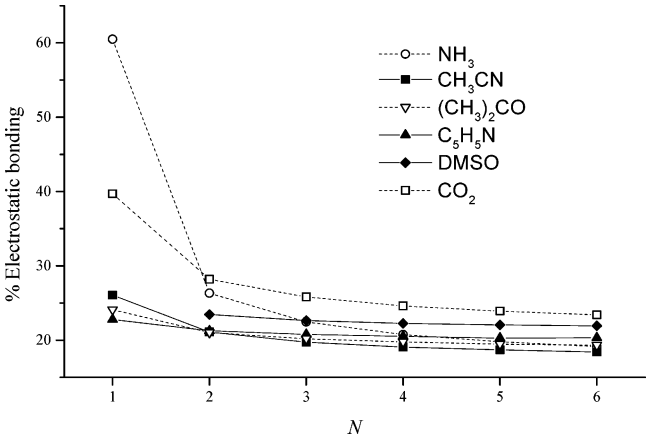

Figure 4. Percentage contribution from electrostatic interactions to the total binding energy of $[AlL_N]^{3+}$ complexes and plotted as a function of the number of ligands (*N*).

show $[Al(H_2O)_N]^{3+}$ complexes to be unstable in the gas phase, with the only ions observed being the hydrolysis products, $[AlOH(H_2O)_N]^{2+}$ and $Al^+(OH)_2(H_2O)_N$.[51−54]

Figure 3 shows a plot of the (NPA) charge calculated to reside on the atom that ligates with Al^{3+} as a function of the number of ligands (note that the data start at $N = 0$, which gives the charge on the atom in the absence of Al^{3+}). In this instance, ammonia does stand out as an example of where the coordinating nitrogen atom retains a high negative charge. In contrast, the calculated results for CO_2 are similar to those seen for acetonitrile and other stabilizing ligands. Given the lack of charge movement on the part of CO_2 (Figure 2) and the high residual negative charge on ammonia ligands (Figure 3), it is not surprising that electrostatic interactions make a significant contribution to bonding in both $[Al(NH_3)_N]^{3+}$ and $[Al(CO_2)_N]^{3+}$ complexes. These results are shown in Figure 4, where it can also be seen that, for efficient electron donors (including acetone), electrostatic interactions make a minor contribution to bonding at all values of *N* studied.

(48) Bock, C. W.; Markham, G. D.; Katz, A. K.; Glusker, J. P. *Inorg. Chem.* **2003**, *42*, 1538−1548.
(49) Wasserman, E.; Rustad, J. R.; Xantheas, S. S. *J. Chem. Phys.* **1997**, *106*, 9769−9780.
(50) Rudolph, W. W.; Mason, R.; Pye, C. C. *Phys. Chem. Chem. Phys.* **2000**, *2*, 5030−5040.
(51) Beyer, M.; Achatz, U.; Berg, C.; Joos, S.; Niedner-Schatteburg, G.; Bondybey, V. E. *J. Phys. Chem. A* **1999**, *103*, 671.
(52) Reinhard, B.; Niedner-Schatteburg, G. *J. Phys. Chem. A* **2002**, *106*, 7988.
(53) Siu, C.-K.; Liu, Z.-F.; Tse, J. S. *J. Am. Chem. Soc.* **2002**, *124*, 10846.
(54) Puskar, L.; Stace, A. J. Unpublished results.

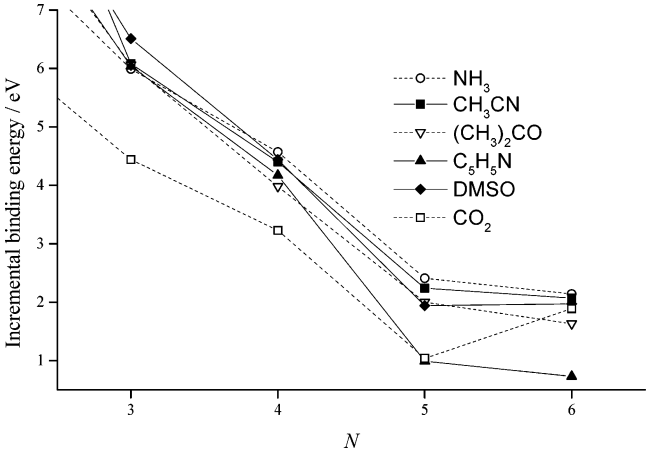

Figure 5. Calculated incremental binding energy in $[AlL_N]^{3+}$ complexes and plotted as a function of the number of coordinating ligands (N). Note that the data start at $N = 3$.

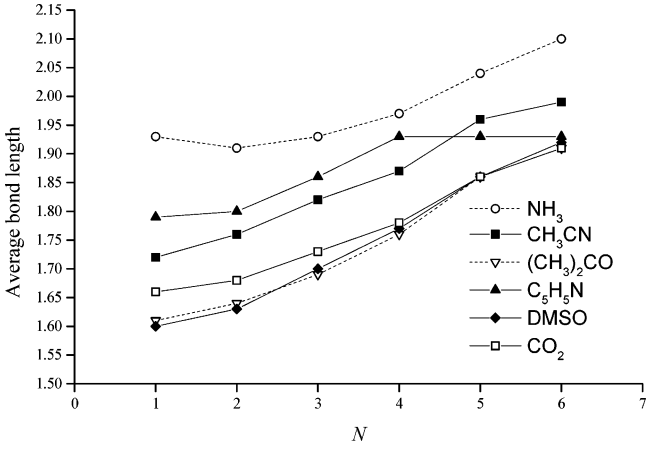

Figure 6. Calculated average bond lengths between the aluminum cation and the ligating atoms. In the case of $[Al(py)_N]^{3+}$ complexes, the data beyond $N = 4$ do not include the extended bond lengths identified in the text.

Table 2. Comparison between Calculated Results on $[AlL_N]^{3+}$ Complexes and Available Experimental Data

complex	experimental bond lengths	calculated bond lengths
$[Al(CH_3CN)_5]^{3+}$ [a]	1.985 (4); 2.021 (1)	1.96 (5)
$[Al(CH_3CN)_6]^{3+}$ [b]	1.91 (4); 1.96 (2)	2.00 (6)[d]
$[Al(DMSO)_6]^{3+}$ [c]	1.894	1.91 (6)

[a] X-ray data taken from ref 19. [b] X-ray data taken from ref 20. [c] EXAFS data taken from ref 49. [d] At some levels of theory, the calculations gave four equivalent bonds and two slightly longer bonds.

Figure 5 shows a plot of the calculated incremental binding energies as a function of N for each of the six different ligands. In this example of behavior in Al^{3+} complexes, carbon dioxide is predicted to be the most weakly bound ligand. When compared with other successful ligands, there appears to be no significant difference in behavior on the part of ammonia. Acetone also has binding energies that compare favorably with those of, for example, acetonitrile. For all of the ligands identified in Figure 5, there are marked changes in binding energy as a function of N, which suggests that complexes with 4-fold coordination (mostly tetrahedral) are particularly stable. By comparison, the addition of further ligands to any of the $[AlL_4]^{3+}$ cations does not lead to a significant enhancement in stability. Indeed, the data for $[Al(py)_N]^{3+}$ show a dramatic decline in binding energy with the addition of a fifth and sixth ligand, to the extent that $[Al(py)_6]^{3+}$ is calculated to be only just stable and, in fact, this species could not be isolated in any of the experiments. These observations, particularly for pyridine, mirror the decline in the ability of additional ligands to donate electron density to Al^{3+} beyond $N = 4$ (see Figure 2). Hence, our suggestion that, for certain bulky ligands in association with very small cations, there may be an *upper limit* to stability in the gas phase.

Finally, for this part of the analysis, Figure 6 presents a plot of the calculated average bond length between the aluminum cation and the coordinating atom on each of the different ligands. The results are given as function of N. In the case of ammonia, these data provide the first evidence of one factor that might contribute to the instability of $[Al(NH_3)_N]^{3+}$ complexes. A comparison between the curve crossing point calculated for ammonia ($R_c = 2.2$ Å) and the bond lengths given in Figure 6 shows that the relatively long $Al^{3+}-N$ distances place all of the complexes within easy reach of the *estimated* charge-transfer separation. Thus, even a comparatively low internal energy could be sufficient to destabilize any of the ammonia-based complexes. In the case of DMSO, the bond length calculated for the $Al^{3+}-O$ bond in $[Al(DMSO)_6]^{3+}$ is 1.91 Å, which is similar than the value of 1.89 Å determined in a recent EXAFS study.[55] Likewise, the calculated $Al^{3+}-N$ bond lengths in $[Al(CH_3CN)_{5,6}]^{3+}$ complexes are similar to those determined from X-ray crystallography.[19,20] These results are summarized in Table 2. The $Al^{3+}-O$ bond distance of 1.71 Å calculated for $[Al(DMSO)_3]^{3+}$ is identical to that determined by El-Nahas et al.[17]

To conclude this preliminary discussion of the results, it would appear that within the data presented thus far, there is no single calculated quantity that correlates directly with the stability of the Al^{3+} complexes listed in Table 1. For carbon dioxide and ammonia, in particular, there are examples in Figures 2−6 where one or another of the ligands does stand out, but there are no instances where together the two molecules exhibit behavior that is markedly different from that of other ligands that form stable complexes. However, in all of the data sets presented in Figures 2−6, the properties identified for acetone do match quite closely those associated with ligands that are known to stabilize Al^{3+}.

In contrast to the simple electrostatic model represented by eqs 7 and 8, the movement of electron density from the ligands on to the metal cation requires the formation of molecular orbitals (MO). Figure 7a shows the MO associated with the HOMO of the tetrahedral structure calculated for $[Al(CH_3CN)_4]^{3+}$, which, as far as the metal cation is concerned, is clearly a nonbonding orbital. Similar behavior is seen for $[Al(py)_4]^{3+}$, where the π orbitals of the aromatic ring contribute to the HOMO, and to a lesser degree for $[Al(Me_2CO)_4]^{3+}$, where the HOMO includes a subset of π orbitals from some of the carbonyl groups. In the case of $[Al(NH_3)_4]^{3+}$, the nonbonding HOMO is made up of contributions from the lone-pair orbitals on the nitrogen atoms. At total energies much lower than that of the HOMO, all six ligands form orbitals of the type shown in Figure 7b for $[Al(CH_3CN)_4]^{3+}$. This is clearly a bonding orbital that involves a strong interaction between σ electrons on each of the ligands and the metal cation. In all of the

(55) Molla-Abbassi, A.; Skripkin, M.; Kritikos, M.; Persson, I.; Mink J.; Sandström, M. *Dalton Trans.* **2003**, 1746−1753.

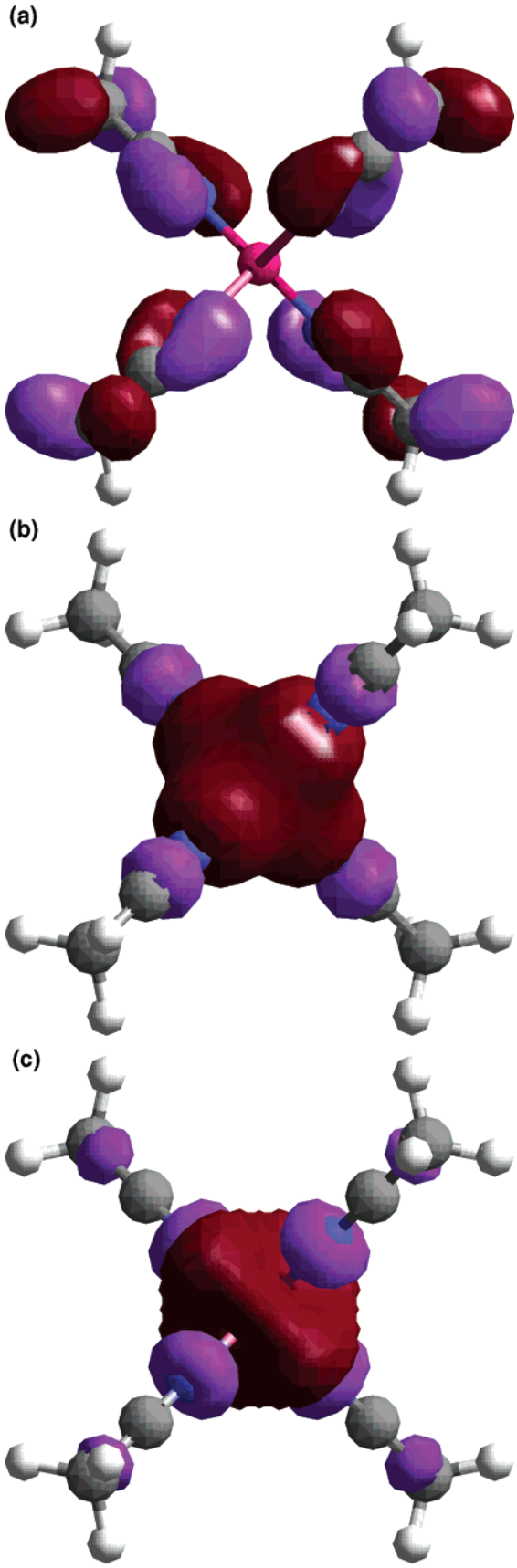

Figure 7. (a) Pictorial representation of the HOMO identified for $[Al(MeCN)_4]^{3+}$; (b) pictorial representation of the bonding orbital (BO) identified for $[Al(MeCN)_4]^{3+}$; (c) pictorial representation of the antibonding orbital (ABO) believed to be responsible for charge transfer in $[Al(MeCN)_4]^{3+}$.

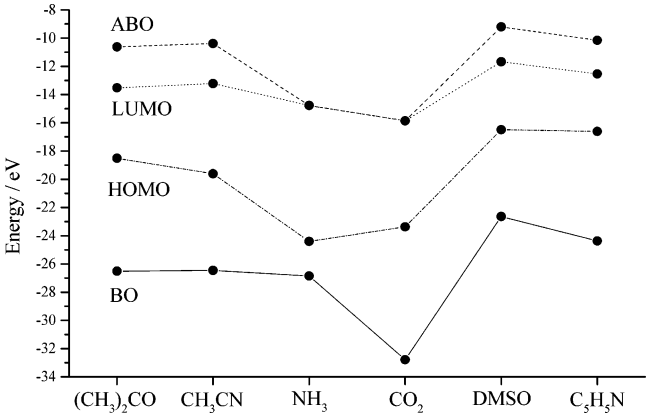

Figure 8. Relative ordering of the energy levels of the various bonding and antibonding orbitals calculated for $[AlL_4]^{3+}$ complexes and plotted for each of the different ligands (L). The exact significance of each type of orbital is discussed in the text.

examples where this type of orbital has been identified, the interaction is associated with every ligand in the complex, thus confirming the view that Al^{3+} is stabilized by powerful σ electron donors. It has also been possible to identify the antibonding (ABO) equivalent of Figure 7b, and an example is shown in Figure 7c. As expected, this orbital is also associated with every ligand in the complex and could be viewed as a possible charge-transfer state. Figure 8 presents a summary of the calculated total energies at which these various orbitals are to be found in $[AlL_4]^{3+}$ complexes, where L is one of the six ligands being evaluated. Also included is the energy of the LUMO, the shape of which has not been the subject of earlier discussion. If instability on the part of a particular $[AlL_4]^{3+}$ combination is equated with the ease of charge (electron) transfer to either the LUMO or the AO, then it is not obvious that the information in Figure 8 helps to differentiate between unstable complexes containing CO_2 and NH_3 and those involving ligands, such as pyridine, that are stable. As can be seen, the energy gap between the HOMO and LUMO for both CO_2 and NH_3 is actually larger than that calculated for pyridine, DMSO, and acetonitrile. However, what is interesting from Figure 8 is the fact that for both CO_2 and NH_3, the antibonding orbital identified in Figure 7c coincides with the LUMO.

(c) NPA and NBO Analysis of Monomeric $[AlL]^{3+}$ Complexes. The significance of the observation regarding the location of the (charge transfer) antibonding orbital is not immediately obvious from the type of calculation performed thus far. However, a natural population analysis of single ligand complexes of the form $[AlL]^{3+}$ helps with the interpretation by revealing the extent to which the *metal cation* can act as both an *electron acceptor* and an *electron donor*, and how the latter process populates ligand orbitals situated just above the HOMO.

Table 3 presents the charge distribution on each $[AlL]^{3+}$ complex in terms of a natural population analysis (NPA) for Al^{3+} together with those atoms on the ligand that are immediately involved with bonding. Charge-transfer contributions from each ligand to the 3s, 3p, and 3d orbitals on Al^{3+} are also given, and these are taken from the effective valence electron configuration ("natural electron configuration") of the metal cation. These contributions show that the metal−ligand interaction primarily involves σ electron donation with a small amount of p and d (π-type interaction) donation. For the case of Al^{3+}−CO_2, the data suggest that the metal−ligand interaction has

Table 3. Natural Population Analysis (NPA) of Al^{3+}–L, Single Ligand Complexes

		Electron Density Donated to Al^{3+}/e				
ligand	Al charge/e	s	p	d	ligand charge/e	
acetonitrile (linear)	2.703	0.20	0.09	0.01	−1.070 N	−0.728 C
acetonitrile (bent)	2.575	0.33	0.09	0.01	−0.985 N	−0.750 C
acetone	2.510	0.33	0.15	0.01	−1.054 O	−0.670 C1,C2
DMSO	2.206	0.58	0.20	0.02	−1.225 O	−0.687 C1,C2
pyridine	2.543	0.41	0.04	0.01	−0.832 N	−0.202 C2,C6
CO_2	2.829	0.07	0.09	0.01	−1.000 O	
NH_3	2.564	0.41	0.02	0.01	−1.200 N	

Table 4. Natural Bond Orbital (NBO) Analysis of the Movement of Electron Density on Al^{3+} (in Units of e^-)

		Back-Donated by Al^{3+} to antibonding orbitals	
ligand	accepted by Al^{3+}	ligand only	metal–ligand
acetonitrile (linear)	0.100	0.034	0.017
acetonitrile (bent)	0.428	0.367	0.395
acetone	0.493	0.088	0.362
DMSO	0.389	0.421	0.392
pyridine	0.427	0.418	0.411
CO_2	0.173	0.021	none
NH_3	0.018	none	0.007

significantly less s character than that which is associated with all of the other ligands, and this, in turn, is reflected in the lack of electron donation to the aluminum cation. Compared with similar calculations by El-Nahas[45] and Peschke et al.[46] on Mg^{2+} (isoelectronic with Al^{3+}),[45] the results show that Al^{3+} is far more effective at attracting electron density from a ligand. Table 4 presents an NBO analysis of the movement of electron density on Al^{3+}, where it can be seen that the cation acts as both an *electron acceptor* and an *electron donor*. The former quantity is determined from the sum of all contributions to Al^{3+} from ligand-only-based orbitals, while electron density donated back to the ligand by Al^{3+} has been split into two categories: (i) donation into antibonding ligand-based orbitals; and (ii) donation into metal-based orbitals on Al^{3+}, which take the form of both metal−ligand antibonding orbitals and valence or Rydberg orbitals on the metal cation. In both Tables 3 and 4, results are presented for two $[AlCH_3CN]^{3+}$ structures, one in which the Al−C−N bond angle is 180° and the other in which the bond is bent at an angle of 163° along the Al−N−C1 bond. It can be seen that the molecule is far more effective as an electron donor when the bond is bent slightly, which may be a consequence of better overlap between the metal cation and donating orbitals on the C≡N group. Likewise, the same structure promotes increased back-donation when compared with the linear configuration. Below, we shall present a more general picture applicable to larger complexes, and under those circumstances, it is possible to revert to the behavior expected of a more realistic linear Al−N−C1 bond.[19,20]

An examination of Table 4 provides our first direct theoretical evidence as to why certain chosen ligands stabilize Al^{3+} and why others that have been selected for calculation (CO_2 and NH_3) fail to do so. It can be seen that two factors distinguish the successful ligands (CH_3CN, etc.) from CO_2 and NH_3, and these include the following: first, the ability to acquire and promote electron density to Al^{3+} valence orbitals, and second,

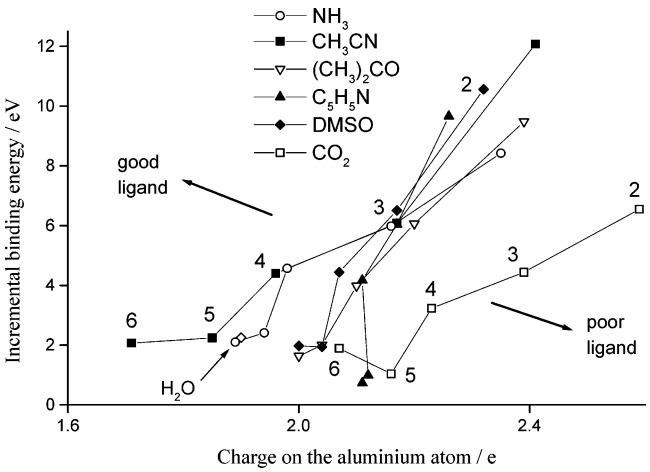

Figure 9. Plot of the calculated incremental binding energy against the calculated charge on the aluminum atom in each of the $[AlL_N]^{3+}$ complexes. Values of *N* are also presented in the figure. A single data point for $[Al(H_2O)_6]^{3+}$ has been taken from ref 48 and is shown as ◇.

the ability to back-donate into ligand antibonding orbitals. If the data in Table 4 are viewed in the context of Figure 8, then it can be seen that all of the successful ligands have an energy gap between the LUMO and the charge-transfer orbital (ABO) depicted in Figure 7c. The calculations show that, within this gap, reside a number of π antibonding orbitals capable of accepting electron density from the metal cation. Therefore, the inability of both CO_2 and NH_3 to stabilize Al^{3+} could be for one or both of the following reasons: first, they promote minimal electron transfer to and from Al^{3+}, and second, if there were a transfer of electron density from the metal to the ligand, then it would go straight into the charge-transfer orbital (ABO) shown in Figure 8. That there is minimal electron transfer between Al^{3+} and either CO_2 or NH_3 in the $[AlL]^{3+}$ complexes underpins the idea that for these two ligands, there is a significant electrostatic contribution to the overall interaction energy (see Figure 4). However, it is necessary to extend these ideas to larger, more realistic structures, and from Figure 2, it can be seen that for $[AlL_4]^{3+}$ complexes, ammonia is as good at donating electron density as any of the more successful ligands (this group now includes complexes with linear Al−acetonitrile bonds). Therefore, the reason for instability comes down to a single factor: *in complexes composed of ligands unable to stabilize Al^{3+}, back-donation from the metal cation to the ligands places electron density into an antibonding, charge-transfer orbital.* If acetone is examined in the context of this statement, then it can be seen from Table 4 that, although it can back-donate electron density, it appears to be the least able to do so, which could also be a source of instability. Similar considerations may also account for the inability of 2-butanone to stabilize Al^{3+}.

Finally, at least two separate studies of bonding between metal dications and ligands of the type discussed here[45,46] have emphasized the relationship between electron transfer from the ligand to the metal and binding energy. Figure 9 summarizes data of that nature for all of ligands studied here; in addition, a single data point has been taken from ref 48 for $[Al(H_2O)_6]^{3+}$. As can be seen, the general trend shows that charge transfer does accompany stability, but that there are notable exceptions. What is evident is that acetonitrile stands out as a good ligand and CO_2 as a poor ligand; however, the plot also implies that

Al^{3+}/ammonia complexes should be stable in the gas phase, which we know is not the case. From the results presented in Figures 2−6, it would appear that there are no unambiguous quantitative criterion for identifying how successful a ligand might be at stabilizing Al^{3+}.

Conclusion

We have shown that it is possible to stabilize Al^{3+} in the gas phase through coordination with comparatively simple ligands. Although ∼30% of the stabilizing interaction is electrostatic in nature, the common features of successful ligands are that they act as good σ electron donors and have a capacity to accept the back-donation of electron density from Al^{3+} into antibonding orbitals. Ligands without this capacity give complexes that are unstable with respect to charge transfer. In view of the successful stabilization of Al^{3+} by acetonitrile, we suggest that compounds with chain or cyclic structures containing −C≡N units could act as successful sequestering agents for Al^{3+}.

Acknowledgment. The authors would like to thank EPSRC for financial support, for the award of an Advanced Fellowship to H.C., and for the award of studentships to K.T. and B.D. We would also like to thank Dr. J. D. Smith for his critical reading of the manuscript and comments on the chemistry of aluminum, and Prof. K. Wade for a number of helpful discussions on bonding in aluminum complexes.

JA042884I